

**Unconfined compressive strength of clay soils at different temperatures
Experimental and constitutive study**

Mohammadi, Fariborz; Maghsoodi, Soheib; Cheshomi, Akbar; Rajabi, Ali M.

DOI

[10.1007/s12665-022-10473-y](https://doi.org/10.1007/s12665-022-10473-y)

Publication date

2022

Document Version

Final published version

Published in

Environmental Earth Sciences

Citation (APA)

Mohammadi, F., Maghsoodi, S., Cheshomi, A., & Rajabi, A. M. (2022). Unconfined compressive strength of clay soils at different temperatures: Experimental and constitutive study. *Environmental Earth Sciences*, 81(15), Article 387. <https://doi.org/10.1007/s12665-022-10473-y>

Important note

To cite this publication, please use the final published version (if applicable).
Please check the document version above.

Copyright

Other than for strictly personal use, it is not permitted to download, forward or distribute the text or part of it, without the consent of the author(s) and/or copyright holder(s), unless the work is under an open content license such as Creative Commons.

Takedown policy

Please contact us and provide details if you believe this document breaches copyrights.
We will remove access to the work immediately and investigate your claim.

Green Open Access added to TU Delft Institutional Repository

'You share, we take care!' - Taverne project

<https://www.openaccess.nl/en/you-share-we-take-care>

Otherwise as indicated in the copyright section: the publisher is the copyright holder of this work and the author uses the Dutch legislation to make this work public.



Unconfined compressive strength of clay soils at different temperatures: experimental and constitutive study

Fariborz Mohammadi¹ · Soheib Maghsoodi² · Akbar Cheshomi¹ · Ali M. Rajabi¹

Received: 21 October 2021 / Accepted: 5 June 2022 / Published online: 23 July 2022
© The Author(s), under exclusive licence to Springer-Verlag GmbH Germany, part of Springer Nature 2022

Abstract

Unconfined compressive strength (S_u) is one of the soil engineering parameters used in geotechnical designs. Due to the temperature changes caused by some human activities, it is important to study the changes in S_u at different temperatures. On the other hand, due to the differences in the mineralogical composition of clay soils, it is important to study this subject in different clays. For this purpose, kaolin, illite and montmorillonite clays with a liquid limit (LL) of 47, 80 and 119, were tested in a temperature-controlled cell in temperature range of 20 to 60 °C. Temperature was applied in undrained conditions and the results showed that the pore water pressure was a function of temperature and by heating, it increased in the samples. For specific temperature pore water pressure generated in montmorillonite was higher than Illite and kaolin. In all three types of clay, the S_u decreased linearly with increasing temperature. The reduction of S_u in kaolin was more than illite and in illite was more than montmorillonite. For all three samples, with increasing temperature, the modulus of elasticity (E) decreased non linearly. Increasing the temperature reduced strength and the stiffness of the clay samples.. The results of unconfined compressive tests at different temperatures were simulated using hypoplastic model. Impact of temperature was replicated by the model.

Keywords Temperature · Unconfined compressive strength (S_u) · Clays · Pore water pressure · Hypoplastic model

Introduction

Human activities, such as disposal of high-level radioactive nuclear wastes, geothermal heat storage, energy geostructures (piles, walls and slabs) and buried high voltage cables, disturb the temperature equilibrium of ground (Brandon et al. 1989; Ghorbani et al. 2020; Lahoori 2020; Lahoori et al. 2021; Maghsoodi 2020; Maghsoodi et al. 2021; Motamedi et al. 2021; Murphy et al. 2015; Tourchi et al. 2021; Bai et al. 2021; Tang et al. 2021). The temperature disturbance may impact the soil physico-mechanical parameters such as shear strength, volumetric behaviour and pore water pressure. Among the mentioned mechanical properties unconfined compressive strength (S_u) of soil is of

great importance due to its application in engineering practice. Theoretically, for saturated clays, the unconfined shear strength and unconsolidated undrained (UU) tests should lead to the same S_u but the unconfined compressive strength is slightly lower than UU tests in practice (Das 2019).

Effect of temperature on mechanical response of clays depends on the heating phase (drained or undrained), stress history (normally consolidated or overconsolidated), clay characteristics (inherent structure, activity, plasticity index,...) and shearing type (drained or undrained, monotonic or cyclic) (Campanella and Mitchell 1968; Hueckel and Baldi 1990; Burghignoli et al. 2000; Cui et al. 2000; Abuel-Naga et al. 2007a; Maghsoodi et al. 2020b, a). Some studies have observed an increase in shear strength, some other reported a decrease, while some have indicated an independence to temperature variations (Abuel-Naga et al. 2007b; Cekerevac and Laloui 2004; Kuntiwattanukul et al. 1995). The uncertainties regarding the impact of temperature on shear strength of clays necessitate more soil element tests under different stress paths (drained and undrained triaxial, unconfined, direct shear).

✉ Akbar Cheshomi
a.cheshomi@ut.ac.ir

¹ College of Science, School of Geology, University of Tehran, Tehran, Iran

² Fugro, The Netherlands formerly Geo-Engineering Section, Faculty of Civil Engineering and Geoscience, Delft University of Technology, Delft, The Netherlands

Undrained heating of normally consolidated clay increases the pore water pressure due to thermal expansion coefficient of the pore fluid which is higher than that of the solid skeleton and this increase continues with keeping the higher temperature constant (Burghignoli et al. 2000; Sulem et al. 2004; Yang et al. 2022). With subsequent cooling the pore pressure decreases. The irreversible volume expansion of saturated soft clay occurs after a heating–cooling cycle, and the irreversible volumetric strain increases with subsequent cycles (Romero et al. 2005; Bai et al. 2014). In overconsolidated clays, undrained heating causes excess pore water pressure (PWP) generation but by keeping the higher temperature constant PWP tends to decrease (Burghignoli et al. 2000; Ghaaowd et al. 2015; Abuel-Naga et al. 2007a; Graham et al. 2001; Monfared et al. 2011, 2014). In drained heating, normally consolidated clays tend to contract which is irreversible in subsequent cooling, while for highly overconsolidated clays dilates upon heating. This dilation is reversible with cooling (Cekerevac and Laloui 2004; Baldi et al. 1988). Li et al. (2021) performed temperature controlled triaxial shear tests on reconstructed marine sediments and with the increasing temperature caused an increase in the slope of the critical state line.

In drained shearing, with increasing temperature, normally consolidated clay contracts and shear strength increases (Sultan et al. 2002). Cekerevac and Laloui (2004) investigated the effect of temperature on the mechanical behaviour of kaolin under drained conditions and the shear strength of NC kaolin clay increased after heating. The same observation has been reported by several authors for NC clays (Abuel-Naga et al. 2007b). On the other hand, in highly overconsolidated clays, different results have been reported in the literature. Some of these studies indicate that the shear stress tends to decrease upon heating (Hueckel and Baldi 1990). They explained this behaviour by the ductile behaviour of the clay during heating. On the contrary, Abuel-Naga et al. 2007b by testing soft Bangkok clay at different temperatures, reported an increase in shear strength of highly OC clays, while the shear stress of kaolin clay with an OCR=12 at 20 and 90 °C were almost the same (Cekerevac and Laloui 2004). Yang et al. (2022) performed thermal consolidation tests on saturated hollow cylindrical silty clay specimens under different temperature and showed that the higher heating or cooling temperature amplitudes, the larger the volumetric strain. They also reported that the volumetric strain decreased with the increase of overconsolidation ratio.

In undrained shearing, Kuntiwattanukul et al. (1995) investigated the effect of temperature on the shear strength of kaolin and they observed that with increasing temperature in NC clay, shear strength increased but in OC clay with increasing temperature, the shear strength remain unchanged. Hueckel and Pellegrini (1992) investigated effect of heating and cooling cycles on the undrained shear

strength of Boom clay and Pontida clay. They concluded that increasing the temperature causes large irreversible strains in the sample.

Extensive research has been carried out to clarify the impact of temperature on friction angle or critical state coefficient (M) of soils. Among these works, Mitchell et al. (2005) reported that, thermal loads would change the inter-particle forces, cohesion and/or friction angle of the soil. On the other hand, Hueckel and Borsetto 1990; Houston and Lin 1987; Graham et al. 2001 and Cekerevac and Laloui 2004 showed that the strength envelope was independent of temperature variations. Hueckel et al. (2009) have explained that the variation of friction angle with temperature may be due to the physico-chemical interactions of clay particles. The thickness of adsorbed water may vary with temperature which changes the contacts between particles. De Bruyn and Thimus (1996) showed with testing Boom-clay at different temperatures and different confining pressures, with heating the soil friction angle decreased. On the other hand, they also observed that the soil cohesion increased with temperature increase while Yu et al. 2018 reported a decrease in cohesion with heating and they also reported that the effect of temperature on the friction angle is not clear. Schuster et al. (2021) showed temperature variation between 20 and 200 °C had negligible effect on the mechanical behavior of Opalinus clay.

Regarding the unconfined compression strength, Sherif and Burrous 1969; Laguros 1969; Murayama 1969; Noble and Demirel 1969 carried out UCS tests on Osaka clay, kaolin, illite and Montmorillonite clay samples in temperature ranges of 20 to 70 °C. They all concluded that with undrained heating, the unconfined compressive strength of clay samples decreased. The reduction of shear strength under heating could be related to the increase in pore water pressure and decrease in effective stress. Sherif and Burrous (1969) mentioned also that the adsorbed water layer around the particles experienced a less rigid state when temperature raised which could be one of the reasons of the strength reduction. Sun et al. (2022) conducted a series of triaxial compression tests on deep sea clay soil subjected to different temperatures. They concluded under drained heating condition, shear strength increased with an increase in temperature. Tomotaka et al. (2020) performed triaxial compression tests under different temperature on silty soils and developed a numerical method for elasto-plastic analysis. Wang et al. (2020b) and Wang et al. (2020a) investigated effects of rate and temperature on the undrained shear behavior of marine clay experimentally and theoretically and proposed an anisotropic thermo-elastic-viscoplastic model. Xiong et al. (2019a) introduced a unified thermo-elasto-plastic model of soils and concluded that the thermomechanical behaviour of soils is mainly controlled by the influence of temperature on the preconsolidation pressure and critical stress ratio.

Among different methods to investigate the shear strength of soils, direct shear test is used extensively in the literature (Vasilescu et al. 2019; Di Donna et al. 2015; Yin 2021; Vafaei et al. 2021; Fakharian and Vafaei 2021; Maghsoodi 2019; Vafaei 2019; Yazdani et al. 2019; Maghsoodi et al. 2020c, 2019 and Xiao et al. 2014). Maghsoodi et al. (2020b) used direct shear test to investigate effect of temperature changes on sand and clay shear strength. Direct shear tests were performed on Fontainebleau sand and kaolin clay. They concluded that the impact of temperature on sandy soil was negligible and the sand behaved thermo-elastic. However, increasing the temperature (22 to 60 °C) in the kaolin clay increased the cohesion and consequently increased the shear strength.

Several constitutive models are proposed to take into account the effect of temperature on mechanical behaviour of soils (Hueckel and Borsetto 1990; Graham et al. 2001; Hueckel et al. 2009; Laloui and François 2009; Hamidi and Khazaei 2010; Yao and Zhou 2013; Mašin and Khalili 2012; Bai and Li 2013; Yao and Zhou 2013; Wang and Qi 2020). Some of these models are based on elasto-plastic approach and some are developed based on hypoplasticity. In recent years, capacity and limitation of these models have been extensively discussed in the literature (Hájek et al. 2009; Wichtmann et al. 2019). Among these models, hypoplastic model, has been extensively used in the literature due to its capacity in good simulation of element tests and boundary value problems and also limited number of parameters (Staubach et al. 2021b, a). Yang et al. (2022) developed the thermodynamic framework of the thermo-hydro-mechanical coupling model of unsaturated clay based on by Yang and Bai (2019) models and showed the modified model can well describe the thermal consolidation behavior of saturated silty clay under different temperature paths. Wang

et al. (2020a) conducted a series of temperature- and rate controlled triaxial tests on marine clay and proposed the anisotropic thermo-elastic-viscoplastic model. Xiong et al. (2019b) presented a thermo-elastoplastic model of normally consolidated and overconsolidated soils based on the modified Cam-clay model and the concept of subloading yield surface.

According to the previous studies, several research has been carried out on the effect of temperature on soil engineering characteristics and different results have been reported. Due to the variety of methods and materials selected, the results obtained from the research have been different. In this regard, in the present study, to investigate the effect of temperature change and soil type on unconfined compressive strength (S_u), three type of clay with different mineralogy were tested at different temperatures and their S_u was determined. For this purpose, a device with the ability to change and keep the temperature constant during the test was designed and manufactured. Afterwards, a hypoplastic model was used to reproduce the experimental results by taking into account the impact of temperature.

Experimental approach

Device description

To investigate the effect of temperature on unconfined compressive strength (S_u) of kaolin, illite and montmorillonite, an apparatus was designed and manufactured. Figure 1 shows the schematic of the apparatus and its various sections.

To raise the temperature in the sample, a Plexiglas cell with high coefficient of thermal resistance was used. The

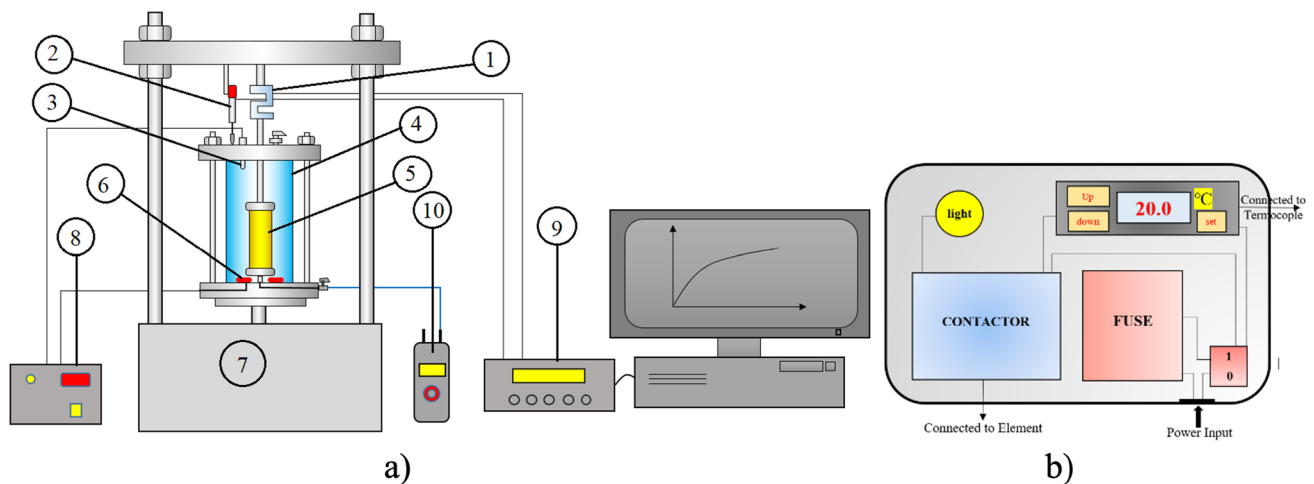


Fig. 1 Schematic of the device and its various components. **a** 1-Load cell, 2-Strain gauge, 3-Temperature sensor, 4-Sample cell, 5-Sample, 6-Element, 7-Loading jack, 8-temperature controlling system, and 9-Data-logger, 10-Digital barometer, **b** Heating/cooling command system

transparency of this cell allows the sample to be seen during the test and how it deforms at different temperatures. The soil sample was placed in the middle of the cell and then the cell was filled with water. Using a circular element located at the bottom of the cell, the water inside the cell was heated to the desired temperature. Temperature was controlled by a thermocouple at the top of the cell. The element set and the thermocouple were connected to a commanding device which displayed and imposed temperature with an accuracy of 0.1 °C. By setting the commanding device to the target temperature, the system could reach the temperature with the imposed rate and kept it constant. To apply the axial strain, a loading frame was used which applied the deformation with a rate of 1 mm/min. To measure the axial force a load cell with measuring capacity of 25 kg force and accuracy of 1 g force was used. This cell allowed to measure the force loaded on the soil sample. To measure the displacement, a LVDT with accuracy of 0.01 mm was used. Data acquisition and display section included a data-logger that recorded and displayed the force measured by load cell and the displacement measured by LVDT. Using the data-logger, it was possible to continuously record force-displacement changes over the time during the test. Pore water pressure measurement section consisted of a digital barometer with an accuracy of 0.01 kPa to measure the pore water pressure of the sample. Thermal calibration was performed on all parts of the device to avoid any device related deformation with heating.

Soil properties

To investigate the effect of clay type and temperature changes, three clay samples (kaolin, illite and montmorillonite) were selected. Figure 2 shows the particle size

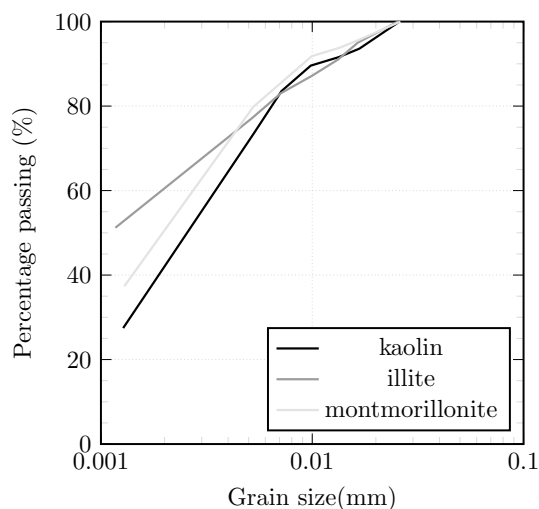


Fig. 2 Grain size distribution of kaolin, illite and montmorillonite

distribution curve of the clays determined according to the standard ASTM 2017b by hydrometric testing. The Atterberg limits and the specific gravity (GS) of the samples were determined according to the standard ASTM 2017a and ASTM 2010, respectively. The activity of the clays based on the method proposed by Skempton (1953) are presented in Table 1.

Table 2 shows the abundance of minerals in the three clay samples based on XRD analysis. In kaolin, about 60% of the mineralogical composition of the sample is kaolinite. The second sample contains about 51% of illite mineral. In the third sample, montmorillonite mineral with 40% abundance is the highest mineral constituent of the sample. Comparing Tables 1 and 2, it can be seen that the difference in the mineralogical composition of the three selected samples has caused differences in the liquid limit (LL), plastic limit (PL) and activity (A) of the samples. So that these three variables have the highest value for montmorillonite sample and the lowest value for kaolin sample. The above variables for the sample contain illite is between the other two samples.

Experimental programme and sample preparation

In this study, unconfined compressive strength of kaolin, illite and montmorillonite samples at different temperatures (20, 30, 40, 50 and 60 °C) were determined based on ASTM (2006). The flowchart of the preparation of soil samples and steps of the test that has been conducted are shown in Fig. 3.

To prepare standard sample (length twice the diameter) and to saturate the samples before the test, a cylindrical mold was made that consisted of two cylinders. The small cylinder contained the clay slurry with two porous stone and the large cylinder had a retaining role. To prepare the samples, the dry powder of sample was mixed with distilled water. The amount of distilled water added to the dry powder of the sample was one and half time the liquid limit (1.5×LL). After stirring the sample and creating a homogeneous slurry, it was poured into the cylindrical sampler. At the top and bottom of the sample, two porous stones were placed and then the sample was consolidated under a vertical stress of 150 kPa which was applied in different increments and was kept for 24 h.

The vertical stress of 150 kPa was selected based on the dimensions of the sampler, the volume of the sample poured into the sampler, sample consistency and the final

Table 1 Clay physical characteristics

	PL%	LL%	PI%	A	G _s
Kaolin	27	47	20	0.48	2.64
Illite	31	80	49	0.82	2.67
Montmorillonite	33	119	86	1.72	2.66

Table 2 Mineral composition characteristics

Clay	Mineral (%)					
	Kaolinite	Illite	Montmorillonite	Quartz	Carbonates	Other
Kaolin	60	2	4	26	2	6
Illite	4	51	–	22	13	10
Montmorillonite	3	3	40	12	20	22

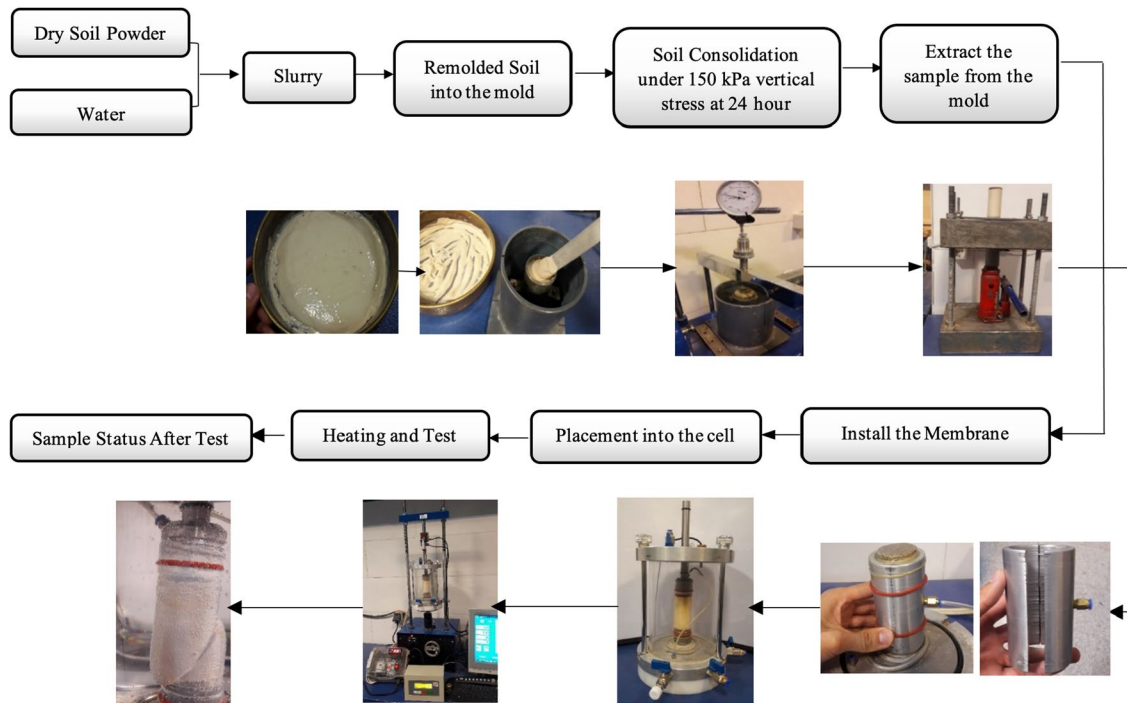


Fig. 3 The sample preparation flowchart and steps of the test that has been conducted

Table 3 Water content, unit weight and void ratio of clays. BC: before consolidation, AC: after consolidation

		ω (%)	γ (kN/m ³)	e
Kaolin	BC*	70	15.6	1.8
	AC**	41	17.6	1.1
Illite	BC	96	14.9	2.4
	AC	63	16.4	1.6
Montmorillonite	BC	143	14.1	3.1
	AC	91	15.7	1.9

desired void ratio of the sample after consolidation. At the end of consolidation phase, based on the dimensions and weight of the sample, the void ratio and degree of saturation of the sample were calculated, which is presented in Table 3. The sample was removed from the sampler using a jack and then a rubber membrane was installed on the sample. To reach the desired temperature, the cell

was filled with water, therefore, the rubber membrane prevented direct contact between the sample and the surrounding water. The sample was then placed inside the cell and then the cell was filled with water. The water inside the cell was heated by the element and the desired temperature was reached using the temperature-control system. Details of the sample preparation process are shown in Fig. 3.

During the heating phase, the upper drainage of the cell was closed and the bottom drainage of sample was connected to the barometer, so the sample was heated in undrained conditions. The heating rate was 5 °C/h.

To ensure uniform heating of the sample, according to the suggestion of Chen et al. (2017), the final temperature was kept constant for 2 h and then the axial load was applied in undrained conditions and the amount of force and displacement was recorded by the data logger. The confining pressure was equal to zero and by applying the axial load (1 mm/min) the sample was sheared in undrained conditions.

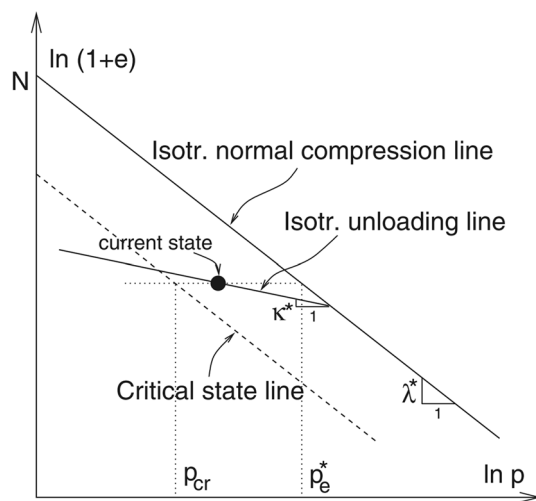


Fig. 4 Parameters of the model (Mašín 2013)

Modeling approach

In this study, the hypoplastic model for clays by Mašín (2005) was used to simulate the experimental results. This model has been thoroughly used and discussed in the literature, therefore, for the sake brevity just some important equations are presented in the appendix. For further readings, readers are referred to Mašín (2013), Mašín (2014), Niemunis (2003) and Gudehus et al. (2008). The general rate formulation of hypoplastic follows:

$$\dot{\sigma} = f_s(\mathcal{L} : \dot{\epsilon} + f_d N || \dot{\epsilon} ||) \quad (1)$$

where $\dot{\sigma}$ and $\dot{\epsilon}$ are the objective stress rate and the Euler stretching tensor, respectively. \mathcal{L} and N are the fourth- and second-order constitutive tensors, f_s and f_d are two scalar factors.

The model has five parameters to be calibrated, ϕ_c , λ , κ , N and ν which have similar (but not the same) interpretation as Modified Cam-clay model parameters. ϕ_c is the critical friction angle of the soil. The slope of the isotropic normal compression line (NCL) in the plane $\ln(1+e)$ vs. $\ln p$; κ is the slope of unloading in the same plane. N is the initial value of $\ln(1+e)$ at the isotropic normal compression line for $p = p_r = 1$ kPa; and finally the parameter ν controls the shear stiffness. These parameters can be observed in Fig. 4.

The implemented hypoplastic model for clays in Brinkgreve and Vermeer (1999) was used to simulate the clay behaviour under uniaxial loading. As has been mentioned by Mašín and Khalili (2012), several parameters of the original hypoplastic model was influenced by temperature variations. In this study, to calibrate the model for different temperatures, trial and error calibration was performed to determine the main parameter which is influenced by the

temperature. Among different parameters of the model, by solely changing N , and keeping other parameters constant, the temperature impact could be simulated. This simple calibration allows to reproduce clay behaviour at different temperatures by only changing one parameter. Mašín and Khalili (2012) proposed the following the equation to consider the impact of temperature on N :

$$\ln(1+e) = N(T) - \lambda^*(T) \frac{p}{p_r} \quad (2)$$

$$N(T) = N + n_T \ln\left(\frac{T}{T_0}\right) \quad (3)$$

where T_0 is the reference temperature and in this study is considered to be 20 °C.

Result and discussion

Consolidation and heating

In the sample preparation step, a vertical stress of 150 kPa was applied to the samples for 24 h to reach the desired void ratio (see Table 3). The water content (ω) and void ratio (e) were 70% and 1.8 before consolidation. These values reduced to $\omega = 41\%$ and $e = 1.1$ after consolidation. For illite, the water content and void ratio before and after consolidation were 96% and 63%, 2.4 and 1.6. For montmorillonite initial water content was 143% which decreased to 91% after consolidation and the void ratios were 3.1 and 1.9, before and after consolidation. Therefore, the percentage of reduction in void ratios for kaolin, illite and montmorillonite samples was 61, 66 and 61, respectively, which is almost the same for the three samples. Figure 5 shows the settlement of the samples versus time. In Fig. 5b–d, the time for 100% of consolidation (t_{100}) was calculated for kaolin, illite and montmorillonite based on the method that have been proposed by Gibson and Henkel (1954). After the determination of the t_{100} using the following equation, the total time of shearing could be calculated. This equation lead to shearing rates related to drained conditions, therefore, rates below the drained conditions can ensure undrained shearing in the samples.

$$t_f = 12.7 \times (t_{100}) \quad (4)$$

The final shearing time in drained conditions for kaolin, illite and montmorillonite was 89, 331 and 368 min. With a shearing rate of 1 mm/min (total shearing time of 27 mins), the undrained shearing conditions is ensured.

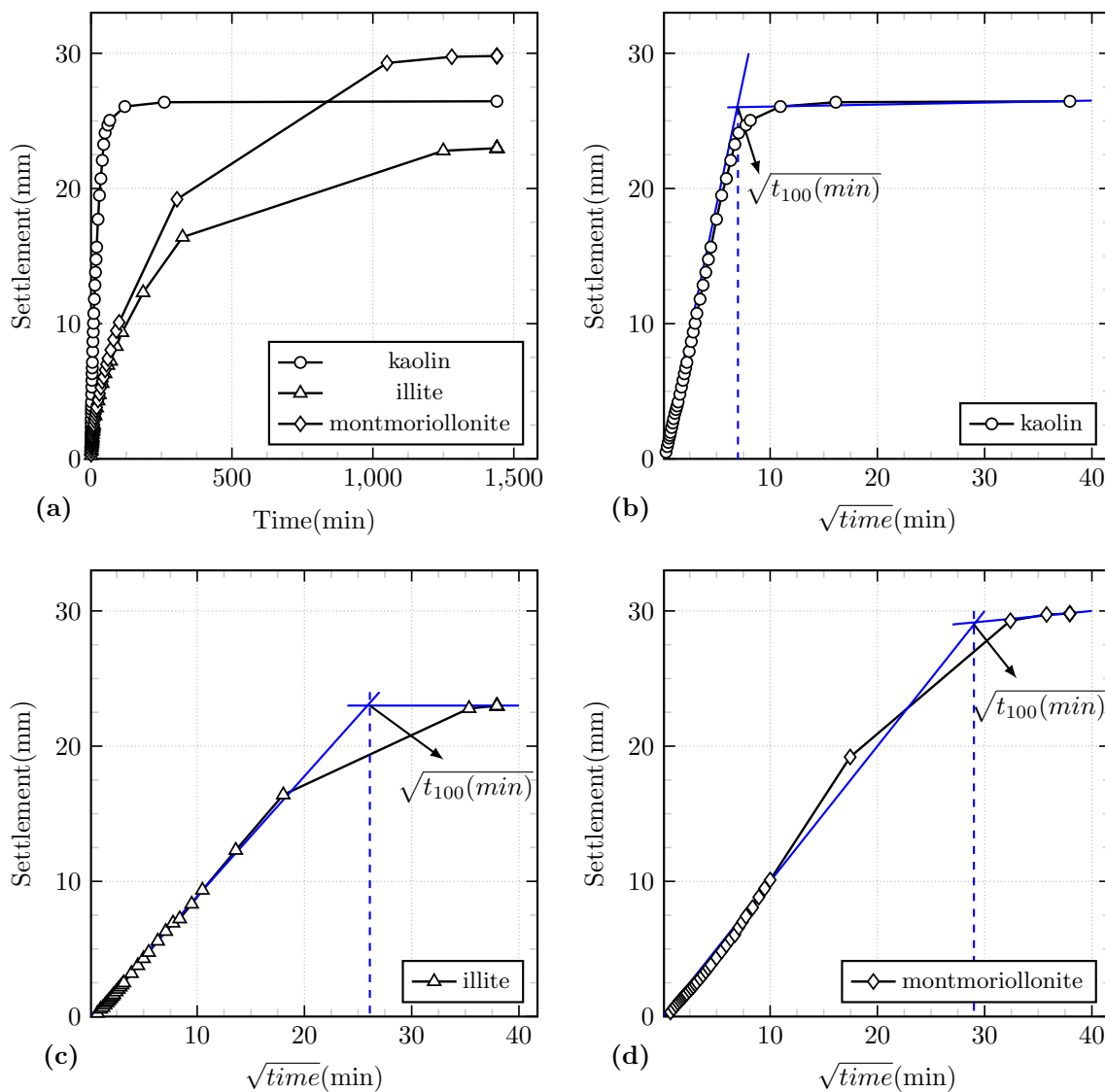


Fig. 5 Time-settlement curve of kaolin, illite and montmorillonite during consolidation phase

The settlement rate for three clay samples was high at the start of loading. The slope of the settlement-time curve for kaolin was steep at first, with the majority of the settlement occurring after 2 h of loading (120 mins). For montmorillonite and illite, this took roughly 20 h (1200 mins). The slope of the settlement-time curves demonstrates that after 24 h under 150 kPa stress, all three specimens reached fully consolidation. Due to the same conditions for all three clays, the difference observed in Fig. 5 could be due to the difference in the type of clay mineral and the permeability of the clays. The slow rate of water drainage in illite and montmorillonite can be attributed to the presence of potassium ions in the illite mineral and the presence of water between the layers of montmorillonite mineral. As a result, the permeability of these two samples was lower than that of kaolin, and the deformation generated by vertical stress occurred at a slower

rate in these two samples than in kaolin. Kaolin has a higher permeability than illite and illite has a higher permeability than montmorillonite, according to the literature (Kobayashi et al. 2017; Mesri and Olson 1971).

Pore water pressure was generated in all three clays during undrained heating. Different reactions of water and solid skeleton to temperature variations led to the generation of pore water pressure with increasing temperature (Burghignoli et al. 2000). Campanella and Mitchell (1968), Agar et al. (1986) and Aversa and Evangelista (1993) showed that under constant confining pressure, the thermally induced pore water pressure corresponds to dilation or contraction of the solid skeleton and the pore water and also the volumetric stiffness of the solid skeleton.

At 20 °C (room temperature), the pore water pressure was zero. The increase in pore water pressure was then measured

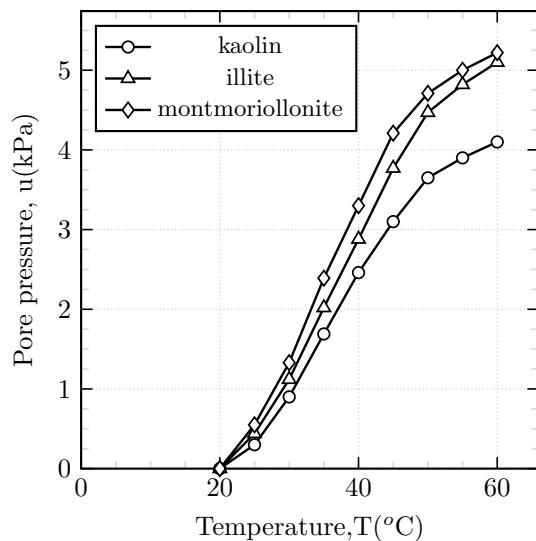


Fig. 6 Pore water pressure generation during heating phase

for every 5 °C of heating. Figure 6 shows that for all three types of clays with increasing temperature, the pore water pressure increased from zero to 4, 5 and 5 kPa for kaolin, illite and montmorillonite. The increase continued until the temperature of about 50 °C and then the rate of increase with temperature was slow down. The slope of the pore water pressure versus temperature was different before and after 50 °C. This slope was higher for temperatures below 50 °C and lower for temperatures above 50 °C.

With a heating rate of 5 °C/h, each heating increment would take 2 h. Figure 7 shows the pore water pressure during heating phase for the three types of clay. The curves show that the higher the temperature during the heating process, the higher the pore water pressure generated in the sample. Furthermore, after 2 h, the pore water pressure in the samples stabilizes. Wang et al. (2020a) and Wang and Qi (2020) reported a same observation. In addition, the heating process will cause the bound water around the soil particles to be activated and converted to free water, which will lead to the soil particle rearrangement and result in volume changes. Moreover, heating will reduce the viscosity of the pore water, increase the permeability coefficient, and make the pore water easier to drain (Towhata et al. 1993).

For kaolin clay the pore water pressure at 30, 40, 50 and 60 °C were 0.9 kPa, 2.46, 3.55 and 4.1 kPa. For illite, each 10 °C (from 20 to 60 °C) of heating generated 1.12, 2.88, 4.47 and 5.1 kPa of pore water pressure. For montmorillonite, the same trend as illite was observed (1.33, 3.30, 4.71 and 5.22 kPa at 30, 40, 50 and 60 °C). In all three clays, the increase in pore water pressure between 50 and 60 °C was less than the other steps. It is worth noting that when illite and montmorillonite are heated to a specific temperature,

the pore water pressure formed is extremely similar to that of kaolin.

Unconfined compressive strength at different temperatures

Prepared and saturated samples according to the method mentioned in the previous section were tested in undrained conditions. Stress-strain curves for kaolin, illite and montmorillonite at 20, 40 and 60 °C are shown in Fig 8a, b and c.

Comparing Fig. 8a, b and c, it can be seen that for different clays, the stress-strain curves are different in terms of shape and the maximum stress value. The shape of the curves indicates the behaviour of the samples at different temperatures and their maximum point indicates the final strength of each sample. At each temperature, several tests were performed and the results were almost similar. For the sake of clarity in the figures, repeatability tests at one temperature for each sample are presented.

The stress-strain curve of kaolin was different from illite and montmorillonite. kaolin curve showed a gradual increase with increasing the axial strain and the rate of shear axial stress decreased after almost 20%. A clear peak was not observed in the stress-strain curve of kaolin. The initial slope of the stress-strain curve in illite and montmorillonite is higher than that of kaolin, and these samples reach their maximum strength at a lower strain level than the kaolin sample after 10% of axial strain they reached a constant stress level, therefore, the tests were stopped. The peak stress is visible in the curves of illite and montmorillonite.

For illite, the initial slope of the stress-strain curve is larger than for montmorillonite and kaolin. While the variation in behavior is dependent on the mineralogical composition of the clays, the difference in behavior is justified based on the LL and water content (ω) in the samples. In the kaolin sample, $\omega = 41\%$ and LL = 47, Therefore, ω of the sample is close to LL. In the illite sample $\omega = 63\%$ and LL = 80 and in the montmorillonite sample, $\omega = 91\%$ and LL = 119. Therefore, there is a difference between ω and the LL in illite and montmorillonite samples. This makes the kaolin sample softer than the other two samples and the slope of its strain-stress curve is less than the other two samples and the maximum point is not seen in its strain-stress curve.

Figure 9 shows the images of failed samples. In kaolin samples, the samples became jar-shaped during the test, and in cases where the failure surface was formed, its angle with the horizon surface was measured at about 45 °. The jar-shaped of the samples is mostly observed at high temperatures. In illite and montmorillonite, unlike kaolin, the jar-shaped was less seen when the samples has been failure, but the angle of the failure surface in them is mostly 45 °. In kaolin, the failure surface is first formed as fine cracks

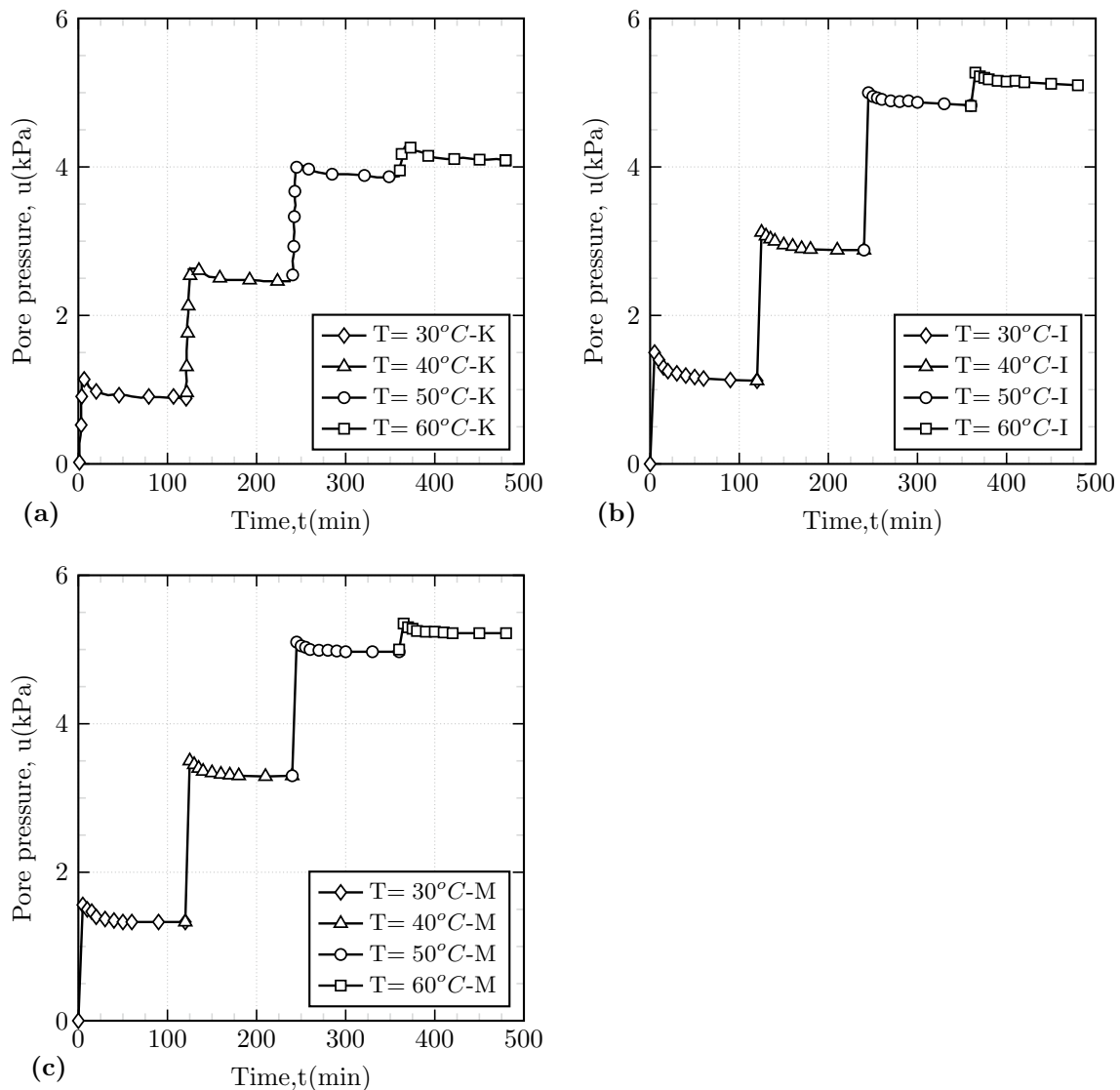


Fig. 7 Pore water pressure generation versus time for each heating stage

and then the main failure surface is formed; But in illite and montmorillonite, the main failure surface is formed immediately and divides the curve into two parts with different slopes.

The maximum stress values for all three samples of stress–strain curves for different temperatures are extracted and shown in Table 4. Changes in S_u versus temperature are plotted in Fig. 10. In all three types of clay, S_u decreases linearly with increasing temperature. S_u for kaolin, illite and montmorillonite decreased from 19.3, 17.4 and 7.1 kPa at 20 °C to 12.5, 11.3 and 4 kPa at 60 °C. The slope of the S_u reduction with temperature is higher for kaolin and illite than for montmorillonite. The slope of S_u reduction for kaolin, illite and montmorillonite were -0.170 , -0.160 and -0.074 . This reduction depends on the soil type, mineralogy, activity and void ratio of clays. It is generally accepted

that the temperature-induced excess pore pressure will lead to the weakness of undrained shear strength for NC clay after undrained heating (Abuel-Naga et al. 2006; Monfared et al. 2012).

Pore water pressure at different temperatures

Figure 11 shows the evolution of pore water pressure during application of axial loading at different temperatures. It can be observed that for kaolin clay, the pore water pressure first increased and then decreased. With increasing temperature, the positive pore water pressure diminished and negative pore water pressure increased. For illite and montmorillonite, the trend was different. For both clays, the pore water pressure increased while shearing. The difference between clays could be attributed to their void ratio after

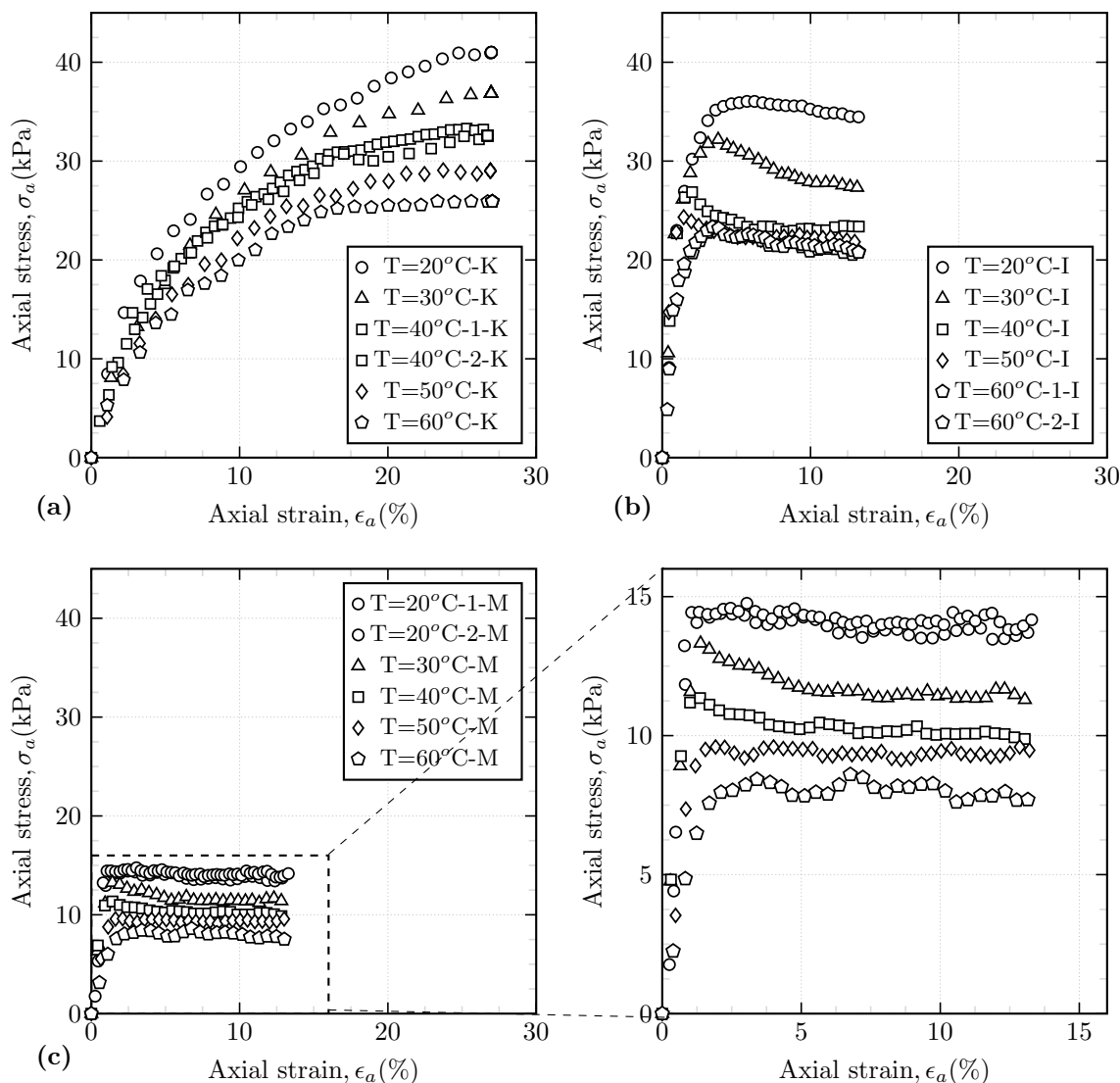


Fig. 8 Changes in S_u versus temperature for all three clay samples

consolidation which was lower in kaolin clay. The lower void ratio in kaolin clay and being in an overconsolidated state, leads to negative pore water pressure. On the contrary for illite and montmorillonite, the void ratios were higher (1.2, 1.6), therefore, they were less stiff compare to kaolin clay and the pore pressure increased while application of axial loading.

The changes in pore water pressure in the heating and shearing process could lead to the decrease in S_u . This subject is consistent with the results of previous study (Campanella and Mitchell 1968; De Bruyn and Thimus 1996; Yu et al. 2018) conducted on saturated clay.

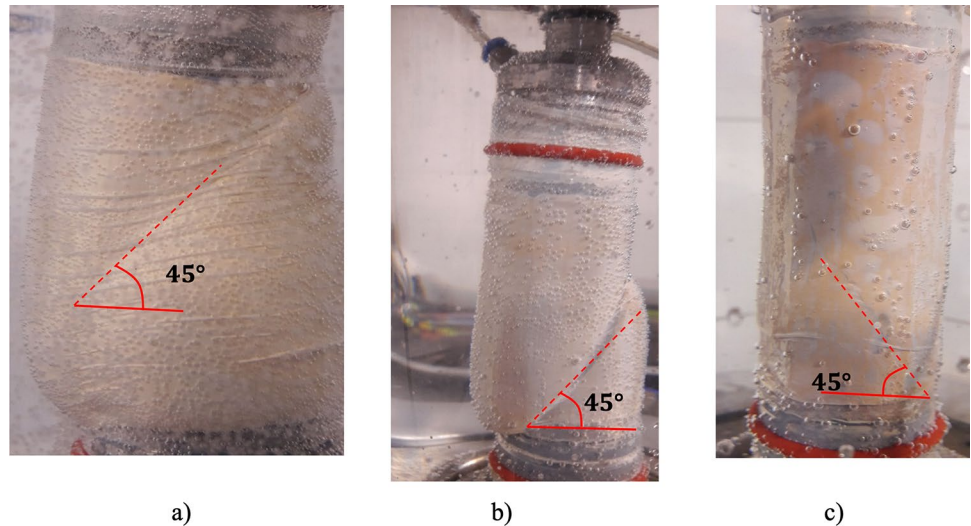
According to the structure of the three studied clay samples, the bonding factor between the sheets in the kaolin is hydrogen bonding and secondary valence forces between the gibbsite and silica sheets. In illite the presence of potassium

ions and in montmorillonite, the weak van der Waals forces and water layers between the sheets (Das 2019). The effect of the increasing temperature on these bonding factors between sheets is different and, therefore, S_u changes with temperature are not the same for the three clays.

Elastic shear modulus

Figure 12 shows the elastic shear modulus for the clays tested at different temperatures. By dividing the axial stress to axial strain in small increments and plot, it against axial strain the evolution of elastic shear modulus can be obtained. As can be seem in Fig. 12a, the elastic shear modulus for kaolin clay at 20 °C started with 8.5 MPa at 0.1% of axial strain and with a slow rate it decreased to 1.5 MPa at 27% of axial strain. With heating, the initial elastic shear modulus

Fig. 9 Failure surface angle in **a** kaolin, **b** illite, **c** montmorillonite



decreased. The initial elastic shear modulus at 40 °C was 8.3 MPa and at 60 °C it again decreased to 7.1 MPa. The rate of reduction for tests at 20 °C is slightly higher than tests at 40 and 60 °C.

Figure 12b shows the evolution of elastic shear modulus for illite. As can be observed the initial elastic modulus at 20 °C started with 28.5 MPa at 0.1 % of axial strain and decreased to 2.6 MPa at 13% of axial strain. Heating decreased the initial elastic modulus from 28.5 to 27 to 25 MPa at 20, 40 and 60 °C respectively. The rate of reduction for 20 and 60 °C was almost similar.

Elastic shear modulus reduction for montmorillonite can be seen in Fig. 12c. The same trend as other clays was observed in this test but the reduction of initial elastic shear modulus at 60 °C was more significant in montmorillonite. The initial elastic modulus at 20 °C was 15.5 MPa and it reduced to 14 and 5.9 at 40 and 60 °C respectively. For all three samples, a decrease in the modulus of elasticity is

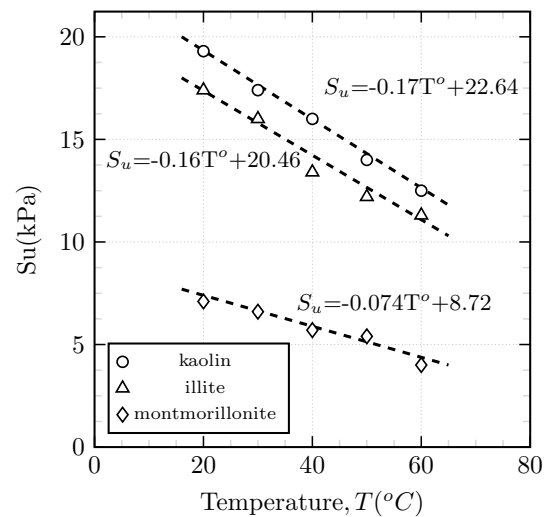


Fig. 10 Changes in S_u versus temperature for all three clay samples

Table 4 Evolution of unconfined compressive strength at different temperatures

T (°C)	S_u (kPa)-kaolin	S_u (kPa)-illite	S_u (kPa)-montmorillonite
20	19.3	17.4	7.1
30	17.4	16	6.6
40	16.1	13.4	5.7
50	14	12.2	5.4
60	12.5	11.3	4

seen with increasing temperature. Increasing the temperature reduces the stiffness of the sample. The slope of the modulus decreases with increasing temperature in three types of clay

is different. The difference in the internal structure of the clays can be the reason for this issue. Decreasing elasticity modulus about 20% as temperature increases from 20 to 60 °C has been reported previously by Zhou and Ng (2013). This subject can be due to thermal softening by increasing temperature (François and Laloui 2008).

Modeling results

To obtain N, calibration was performed at 20 and 60 °C then by extrapolating the values corresponding to 30 40 and 50 °C were obtained. The trend of N with $\ln T/T_0$ is illustrated in Fig. 13 for the clays. Similar reductive trend of N with $\ln T/T_0$ has been reported by Mašin and Khalili (2012).

Using the parameters shown in Table 5, the unconfined compressive test for clays at different temperatures was

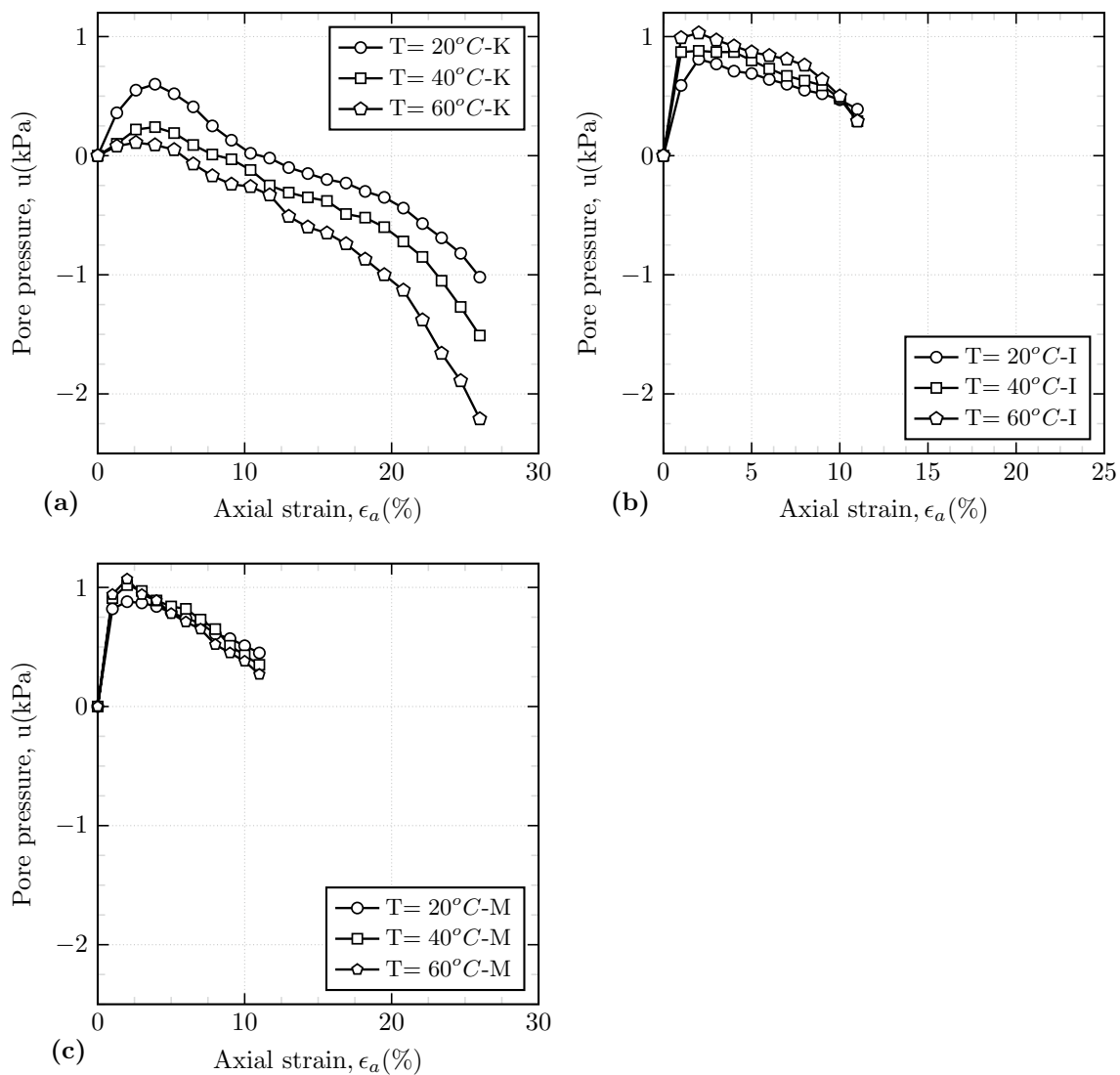


Fig. 11 Evolution of pore water pressure during axial loading

simulated. Figure 14 illustrates the modelling simulation against experimental results. For all of the simulations, the parameters were calibrated against tests at 20°C and by changing N the model capacity was examined for the tests at other temperatures (30°C , 40°C , 50°C and 60°C). For kaolin clay, the same friction angle (21°) as Mašín (2013) was selected as input parameter. The other parameters ($\lambda^* = 0.055$, $\kappa^* = 0.0195$, $N_{20^\circ\text{C}} = 0.995$, $N_{60^\circ\text{C}} = 0.970$ and $\nu/r = 0.7$) was found by tuning the values proposed by Gudehus et al. (2008) for these clays. It can be observed the initial stiffness reproduced by the model up to an axial strain of 5% was slightly higher than experimental results at 50°C and 60°C but the overall trend and particularly the axial stress at large axial strains ($> 10\%$) of stress–strain curve was well reproduced by the model.

For illite, the model parameters were found to be $\phi_c = 22^\circ$, $\lambda^* = 0.075$, $\kappa^* = 0.0090$, $N_{20^\circ\text{C}} = 1.287$, $N_{60^\circ\text{C}} = 1.248$ and $\nu/r = 0.2$. For tests at 30°C , 40°C , 50°C and 60°C the peak stress was not replicated by the model but the stress corresponds to larger strains were reproduced correctly by the model (Fig. 14b).

Simulations are in good agreement for montmorillonite results at different temperatures (Fig. 14c). The friction angle in the model was 22° , λ^* was found to be 0.070, κ^* was 0.012 and ν/r was equal to 0.3. By decreasing N from 1.310 (20°C) to 1.270 (60°C), impact of temperature could be reproduced. The initial stiffness reproduced by the model was slightly lower than experimental results for tests at 20°C , 30°C and 40°C .

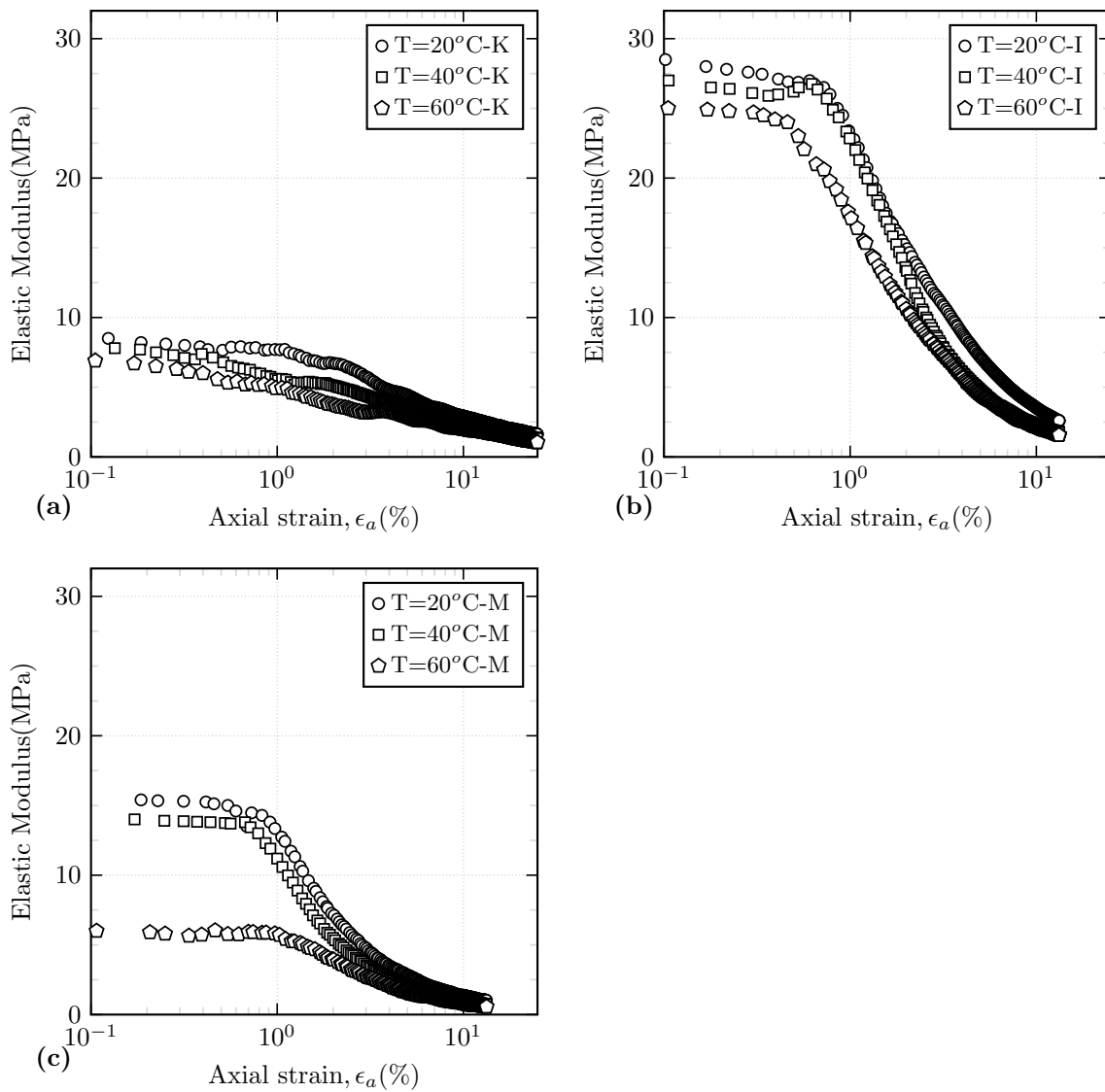


Fig. 12 Secant shear modulus reduction during axial loading for different temperatures

Conclusions

To investigate the effect of temperature on unconfined compressive strength of clays, a cell with the ability to increase the temperature was considered and experiments in undrained conditions with cell pressure equal zero on three types of clay (illite, kaolin and montmorillonite) under saturated conditions at temperatures of 20, 30, 40, 50 and 60 °C were carried out and afterwards using hypoplastic model for clays, the experimental results were replicated with implementing the impact of temperature in the constitutive formulation. The following remarks can be mentioned:

- In three clays during undrained heating due to different reactions of water and solid skeleton to temperature, by increasing temperature, the pore water pressure increases.

The shape of the pore water pressure–temperature curve is similar for the three samples, and the curve for the montmorillonite sample is higher than illite and illite is higher than kaolin.

- With increasing temperature for three soil samples, the unconfined compressive strength decreased linearly. The reason for this decrease was the increase of pore water pressure due to heating. Due to the differences in the mineralogical composition of the studied soils, the mentioned reduction was different for different clay soils. Increasing the temperature from 20 to 60 °C reduced the strength by 35, 35 and 43% for kaolin, illite and montmorillonite, respectively.
- Increasing temperature reduced the initial elastic modulus in three types of clay.

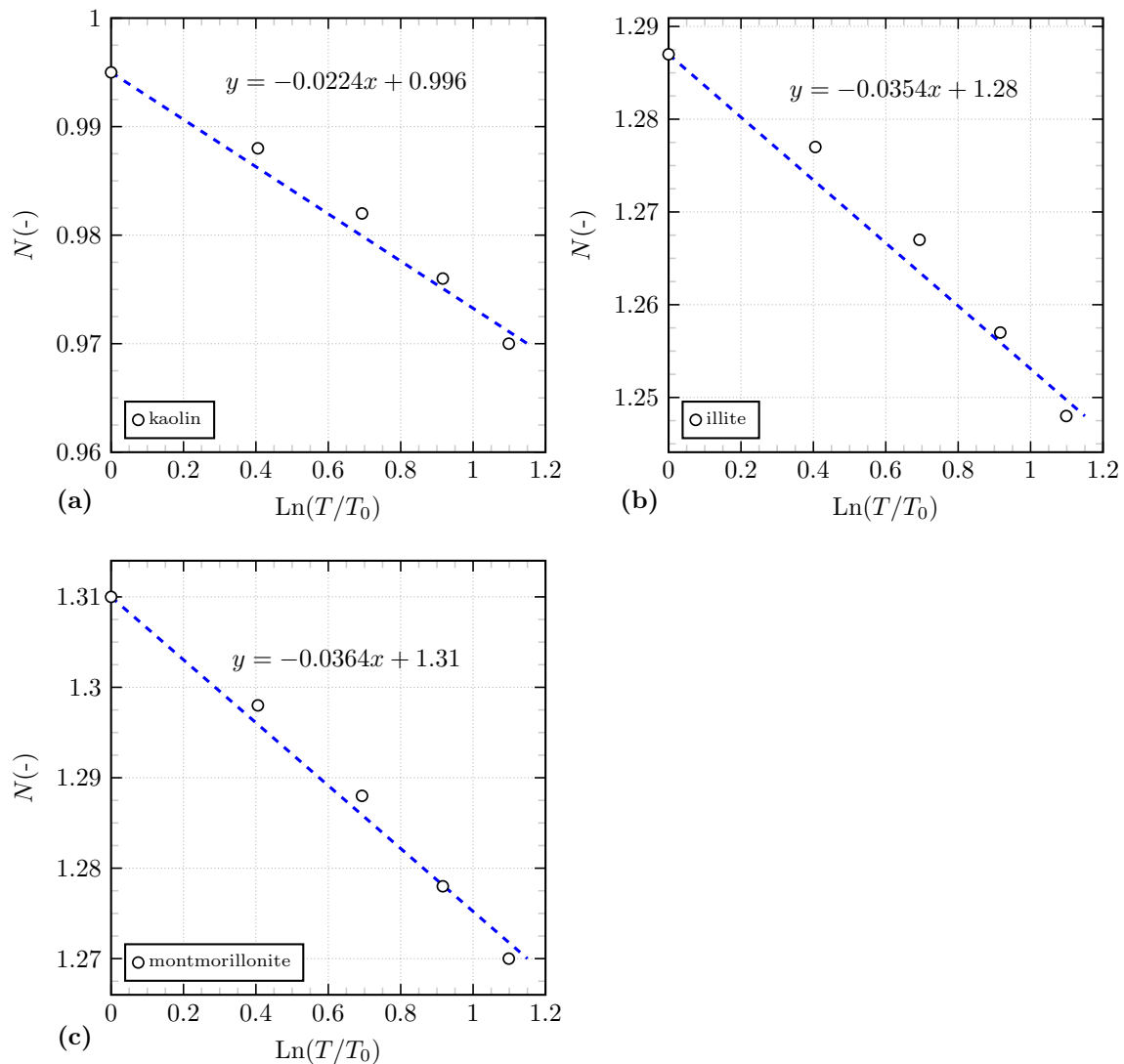


Fig. 13 Evolution of N with $\ln(T/T_0)$

- The stress–strain curve of kaolin at different temperatures had no peak, while for illite and montmorillonite samples a clear peak at strains around 2% was observed.
- In the heating phase with a rate of 5 °C/h, the pore water pressure in the samples increased. The increase in pore water pressure in illite and montmorillonite was greater than kaolin.
- During the application of axial loading, the pore water pressure in kaolin first slightly increased and then decreased. In illite and montmorillonite, the increase in pore water pressure at the beginning of the axial loading was greater than in kaolin.
- The different reactions of the three types of clays tested in the present study to temperature changes depend on their inherent structure. This different internal structure causes the permeability of the tested clays to be different. In addition, it causes a difference in the pore water pressure created and eliminated in the samples. Uniaxial strength and modulus of elasticity of samples at different temperatures are affected by the pore water pressure.
- Using single set of parameters for each soil, by taking into account the impact of temperature on the initial void ratio of the samples, the hypoplastic model replicated the experimental results with good agreement.

Further studies should be carried out to investigate the undrained shear strength of these clays in triaxial device at different temperatures to compare the results with unconfined tests.

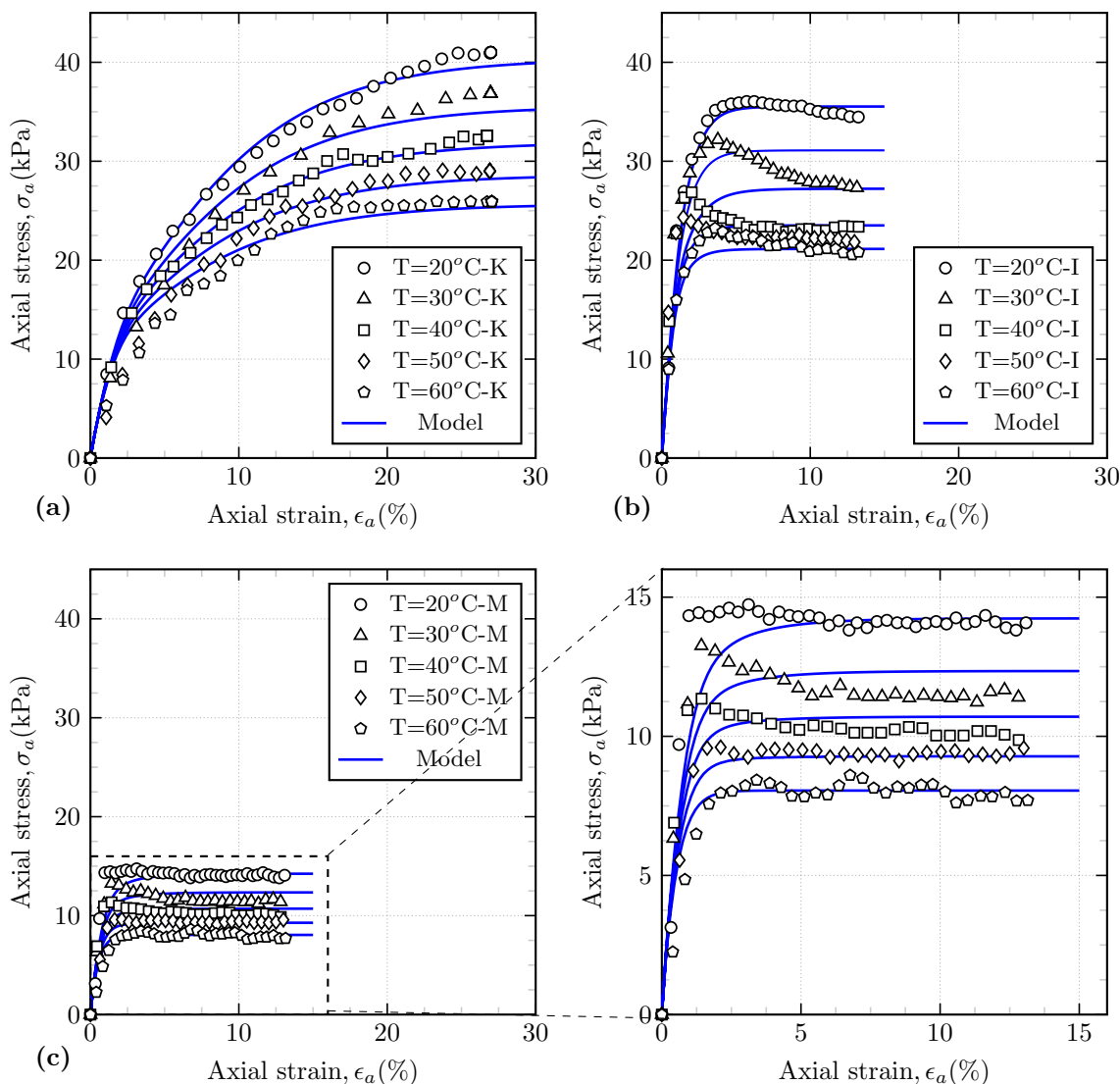


Fig. 14 Hypoplastic simulations against experimental results

Table 5 Hypoplastic model parameters used in this study

Soil	ϕ_c	λ^*	κ^*	$N_{20^\circ C}$	$N_{60^\circ C}$	ν/r
Kaolin	21	0.055	0.0195	0.995	0.970	0.7
Illite	18.7	0.075	0.009	1.287	1.248	0.2
Montmorillonite	18	0.070	0.012	1.31	1.27	0.3

Appendix

Formulation of the hypoplastic model is as follows (Mašín 2013):

$$\dot{\mathbf{T}} = f_s \mathcal{L} : \mathbf{D} \frac{f_d}{f_a} \mathcal{A} : \mathbf{d} ||\mathbf{D}|| \tag{5}$$

with

$$\mathcal{L} = \mathcal{I} + \frac{\nu}{1-2\nu} \mathbf{1} \otimes \mathbf{1} \tag{6}$$

$$\mathcal{A} = f_s \mathcal{L} + \frac{\mathbf{T}}{\lambda^*} \otimes \mathbf{1} \tag{7}$$

$$f_s = \frac{3p}{2} \left(\frac{1}{\lambda^*} + \frac{1}{\kappa^*} \right) \frac{1-2\nu}{1+\nu} \tag{8}$$

where ν , λ^* and κ^* are model parameters, $p = -\text{tr}\mathbf{T}/3$, and $\mathbf{1}$ and \mathcal{I} are second- and fourth-order unity tensors, respectively. The factor f_d reads

$$f_d = \left(\frac{2p}{p_e} \right)^\alpha \quad (9)$$

with $\alpha = 2$ and the equivalent pressure

$$p_e = p_r \exp \left[\frac{N - \ln(1 + e)}{\lambda^*} \right] \quad (10)$$

where N is a parameter and p_r is a reference stress equal to 1 kPa. The factor f_d^A reads

$$f_d^A = 2^\alpha (1 - F_m)^{\alpha/\omega} \quad (11)$$

where F_m is the Matsuoka-Nakai factor calculated from

$$F_m = \frac{9I_3 + I_1 I_2}{I_3 + I_1 I_2} \quad (12)$$

and the exponent ω reads

$$\omega = -\frac{\ln(\cos^2 \phi_c)}{\ln 2} + a(F_m - \sin^2 \phi_c) \quad (13)$$

$$I_1 = \text{tr}\mathbf{T} \quad (14)$$

$$I_2 = \frac{1}{2} [\mathbf{T} : \mathbf{T} - (I_1)^2] \quad (15)$$

$$I_3 = \det \mathbf{T} \quad (16)$$

Finally, the asymptotic strain rate direction \mathbf{d} is calculated as

$$\mathbf{d} = \frac{\mathbf{d}^A}{\|\mathbf{d}^A\|} \quad (17)$$

$$\mathbf{d} = -\hat{\mathbf{T}}^* + 1 \left[\frac{2}{3} - \frac{\cos 3\theta + 1}{4} F_m^{1/4} \right] \frac{F_m^{\zeta/2} - \sin^\zeta \phi_c}{1 - \sin^\zeta \phi_c} \quad (18)$$

with the Lode angle θ

$$\cos 3\theta = -\sqrt{6} \frac{\text{tr}(\hat{\mathbf{T}}^* \cdot \hat{\mathbf{T}}^* \cdot \hat{\mathbf{T}}^*)}{[\hat{\mathbf{T}}^* : \hat{\mathbf{T}}^*]^{3/2}} \quad (19)$$

exponent ζ

$$\zeta = 1.7 + 3.9 \sin^2 \phi_c \quad (20)$$

and the stress measure $\hat{\mathbf{T}}^* = \mathbf{T}/\text{tr}\mathbf{T} - \mathbf{1}/3$. The model requires five parameters ϕ_c , λ , κ , N and ν , and state variables \mathbf{T} and void ratio e .

References

- Abuel-Naga H, Bergado D, Ramana G, Grino L, Rujvivipat P, Thet Y (2006) Experimental evaluation of engineering behavior of soft Bangkok clay under elevated temperature. *J Geotech Geoenviron Eng* 132(7):902–910
- Abuel-Naga HM, Bergado DT, Bouazza A (2007) Thermally induced volume change and excess pore water pressure of soft Bangkok clay. *Eng Geol* 89(1–2):144–154
- Abuel-Naga HM, Bergado DT, Lim BF (2007) Effect of temperature on shear strength and yielding behavior of soft Bangkok clay. *Soils Found* 47(3):423–436
- Agar J, Morgenstern N, Scott J (1986) Thermal expansion and pore pressure generation in oil sands. *Can Geotech J* 23(3):327–333
- ASTM (2006) Standard test method for unconfined compressive strength of cohesive soil. ASTM D2166, West Conshohocken, PA
- ASTM (2010) Standard test methods for specific gravity of soil solids by water pycnometer. ASTM 854–14, West Conshohocken, PA
- ASTM (2017) standard test method for liquid limit, plastic limit, and plasticity index of soils. ASTM D4318, West Conshohocken, PA
- ASTM (2017) Standard test method for particle-size analysis of soils. ASTM D422–63, West Conshohocken, PA
- Aversa S, Evangelista A (1993) Thermal expansion of neapolitan yellow tuff. *Rock Mech Rock Eng* 26(4):281–306
- Bai B, Guo L, Han S (2014) Pore pressure and consolidation of saturated silty clay induced by progressively heating/cooling. *Mech Mater* 75:84–94
- Bai B, Li T (2013) Irreversible consolidation problem of a saturated porothermoelastic spherical body with a spherical cavity. *Appl Math Model* 37(4):1973–1982
- Bai B, Nie Q, Zhang Y, Wang X, Hu W (2021) Cotransport of heavy metals and SiO_2 particles at different temperatures by seepage. *J Hydrol* 597:125771
- Baldi G, Hueckel T, Pellegrini R (1988) Thermal volume changes of the mineral-water system in low-porosity clay soils. *Can Geotech J* 25(4):807–825
- Brandon T, Mitchell J, Cameron J (1989) Thermal instability in buried cable backfills. *J Geotech Eng* 115(1):38–55
- Brinkgreve RB, Vermeer P (1999) *Plaxis: finite element code for soil and rock analyses: version 7:[user's guide]*. Balkema, Avereest
- Burghignoli A, Desideri A, Miliziano S (2000) A laboratory study on the thermomechanical behaviour of clayey soils. *Can Geotech J* 37(4):764–780
- Campanella RG, Mitchell JK (1968) Influence of temperature variations on soil behavior. *J Soil Mech Found Div* 94(SM3):709–734
- Cekerevac C, Laloui L (2004) Experimental study of thermal effects on the mechanical behaviour of a clay. *Int J Numer Anal Methods Geomech* 28(3):209–228. <https://doi.org/10.1002/nag.332>
- Chen W, Ma Y, Yu H, Li F, Li X, Sillen X (2017) Effects of temperature and thermally-induced microstructure change on hydraulic conductivity of boom clay. *J Rock Mech Geotech Eng* 9(3):383–395
- Cui YJ, Sultan N, Delage P (2000) A thermomechanical model for saturated clays. *Can Geotech J* 37(3):607–620
- Das BM (2019) *Advanced soil mechanics*. CRC Press, New York
- De Bruyn D, Thimus J-F (1996) The influence of temperature on mechanical characteristics of boom clay: the results of an initial laboratory programme. *Eng Geol* 41(1–4):117–126
- Di Donna A, Ferrari A, Laloui L (2015) Experimental investigations of the soil-concrete interface: physical mechanisms, cyclic mobilization, and behaviour at different temperatures. *Can Geotech J* 53(4):659–672
- Fakharian K, Vafaei N (2021) Effect of density on skin friction response of piles embedded in sand by simple shear interface tests. *Can Geotech J* 58(5):619–636

- François B, Laloui L (2008) Acmeq-ts: A constitutive model for unsaturated soils under non-isothermal conditions. *Int J Numer Anal Meth Geomech* 32(16):1955–1988
- Ghaaowd I, Takai A, Katsumi T, McCartney JS (2015) Pore water pressure prediction for undrained heating of soils. *Environ Geotech* 4(2):70–78
- Ghorbani B, Arulrajah A, Narsilio G, Horpibulsuk S (2020) Experimental and ann analysis of temperature effects on the permanent deformation properties of demolition wastes. *Transp Geotech* 24:100365
- Gibson R, Henkel D (1954) Influence of duration of tests at constant rate of strain on measured “drained” strength. *Géotechnique* 4(1):6–15
- Graham J, Tanaka N, Crilly T, Alfaro M (2001) Modified cam-clay modelling of temperature effects in clays. *Can Geotech J* 38(3):608–621
- Gudehus G, Amorosi A, Gens A, Herle I, Kolymbas D, Mašín D, Muir Wood D, Niemunis A, Nova R, Pastor M et al (2008) The soilmodels. info project. *Int J Numer Anal Meth Geomech* 32(12):1571–1572
- Hájek V, Mašín D, Boháč J (2009) Capability of constitutive models to simulate soils with different ocr using a single set of parameters. *Comput Geotech* 36(4):655–664
- Hamidi , Khazaei C (2010) A thermo-mechanical constitutive model for saturated clays. *Int J Geotech Eng* 4:445–459
- Houston SL, Lin H-D (1987) A thermal consolidation model for pelagic clays. *Mar Georesour Geotechnol* 7(2):79–98
- Hueckel T, Baldi G (1990) Thermoplasticity of saturated clays: experimental constitutive study. *J Geotech Eng* 116(12):1778–1796
- Hueckel T, Borsetto M (1990) Thermoplasticity of saturated soils and shales: constitutive equations. *J Geotech Eng* 116(12):1765–1777
- Hueckel T, François B, Laloui L (2009) Explaining thermal failure in saturated clays. *Géotechnique* 59(3):197–212
- Hueckel T, Pellegrini R (1992) Effective stress and water pressure in saturated clays during heating-cooling cycles. *Can Geotech J* 29(6):1095–1102
- Kobayashi I, Owada H, Ishii T, Iizuka A (2017) Evaluation of specific surface area of bentonite-engineered barriers for kozeny-carman law. *Soils Found* 57(5):683–697
- Kuntiwattanakul P, Towhata I, Ohishi K, Seko I (1995) Temperature effects on undrained shear characteristics of clay. *Soils Found* 35(1):147–162
- Laguros JG (1969) Effect of temperature on some engineering properties of clay soils. *Highway Res Board Spec Rep* (103)
- Lahoori M (2020) Thermo-hydro-mechanical behavior of an embankment to store thermal energy. PhD thesis, Université de Lorraine
- Lahoori M, Rosin-Paumier S, Masrouri F (2021) Effect of monotonic and cyclic temperature variations on the mechanical behavior of a compacted soil. *Eng Geol* 290:106195
- Laloui L, François B (2009) Acmeq-t: soil thermoplasticity model. *J Eng Mech* 135(9):932–944
- Li H, Kong G, Wen L, Yang Q (2021) Pore pressure and strength behaviors of reconstituted marine sediments involving thermal effects. *Int J Geomech* 21(4):06021008
- Maghsoodi S (2019) L’effet de la température sur le comportement thermomécanique de l’interface sol-structure. *Acad J Civ Eng* 37(1):333–338
- Maghsoodi S (2020) Thermo-mechanical behavior of soil-structure interface under monotonic and cyclic loads in the context of energy geostructures. PhD thesis, Université de Lorraine
- Maghsoodi S, Cuisinier O, Masrouri F (2019) Comportement thermomécanique de l’interface sable-structure. In: 17th European Conference on Soil Mechanics and Geotechnical Engineering
- Maghsoodi S, Cuisinier O, Masrouri F (2020) Effect of temperature on the cyclic behavior of clay-structure interface. *J Geotech Geoenviron Eng* 146(10):04020103
- Maghsoodi S, Cuisinier O, Masrouri F (2020) Thermal effects on mechanical behaviour of soil-structure interface. *Can Geotech J* 57(1):32–47
- Maghsoodi S, Cuisinier O, Masrouri F (2020c) Thermal effects on one-way cyclic behaviour of clay-structure interface, E3S Web Conf 205, EDP Sciences, p 05001
- Maghsoodi S, Cuisinier O, Masrouri F (2021) Non-isothermal soil-structure interface model based on critical state theory. *Acta Geotech* 16(7):2049–2069
- Mašín D (2005) A hypoplastic constitutive model for clays. *Int J Numer Anal Meth Geomech* 29(4):311–336
- Mašín D (2013) Clay hypoplasticity with explicitly defined asymptotic states. *Acta Geotech* 8(5):481–496
- Mašín D (2014) Clay hypoplasticity model including stiffness anisotropy. *Géotechnique* 64(3):232–238
- Mašín D, Khalili N (2012) A thermo-mechanical model for variably saturated soils based on hypoplasticity. *Int J Numer Anal Meth Geomech* 36(12):1461–1485
- Mesri G, Olson RE (1971) Mechanisms controlling the permeability of clays. *Clays Clay Miner* 19(3):151–158
- Mitchell JK, Soga K et al (2005) *Fundamentals of soil behavior*, vol 3. Wiley, New York
- Monfared M, Sulem J, Delage P, Mohajerani M (2011) A laboratory investigation on thermal properties of the opalinus claystone. *Rock Mech Rock Eng* 44(6):735
- Monfared M, Sulem J, Delage P, Mohajerani M (2012) On the thm behaviour of a sheared boom clay sample: Application to the behaviour and sealing properties of the edz. *Eng Geol* 124:47–58
- Monfared M, Sulem J, Delage P, Mohajerani M (2014) Temperature and damage impact on the permeability of opalinus clay. *Rock Mech Rock Eng* 47(1):101–110
- Motamedi Y, Makasis N, Gu X, Narsilio GA, Arulrajah A, Horpibulsuk S (2021) Investigating the thermal behaviour of geothermal pavements using thermal response test (trt). *Transp Geotech* 29:100576
- Murayama S (1969) Effect of temperature on elasticity of clays. *Highway research board special report* (103)
- Murphy KD, McCartney JS, Henry KS (2015) Evaluation of thermo-mechanical and thermal behavior of full-scale energy foundations. *Acta Geotech* 10(2):179–195
- Niemunis A (2003) *Extended hypoplastic models for soils*, Vol. 34, Inst. für Grundbau und Bodenmechanik
- Noble CA, Demirel T (1969) Effect of temperature on strength. *Spec Rep* (103):204
- Romero E, Villar M, Lloret A (2005) Thermo-hydro-mechanical behaviour of two heavily overconsolidated clays. *Eng Geol* 81(3):255–268
- Schuster V, Rybacki E, Bonnelye A, Herrmann J, Schleicher AM, Dresen G (2021) Experimental deformation of opalinus clay at elevated temperature and pressure conditions: Mechanical properties and the influence of rock fabric. *Rock Mech Rock Eng* 54(8):4009–4039
- Sherif MA, Burrous CM (1969) Temperature effects on the unconfined shear strength of saturated, cohesive soil. *Effects Temp Heat Eng Behav Soils Spec Rep* 103:267–272
- Skempton A (1953) The colloidal activity of clays. *Select Pap Soil Mech* pp 106–118
- Staubach P, Machaček J, Sharif R, Wichtmann T (2021) Back-analysis of model tests on piles in sand subjected to long-term lateral cyclic loading: Impact of the pile installation and application of the hca model. *Comput Geotech* 134:104018
- Staubach P, Machaček J, Wichtmann T (2021) Large-deformation analysis of pile installation with subsequent lateral loading: Sanisand vs. hypoplasticity. *Soil Dyn Earthq Eng* 151:106964

- Sulem J, Vardoulakis I, Ouffroukh H, Boulon M, Hans J (2004) Experimental characterization of the thermo-poro-mechanical properties of the aegion fault gouge. *CR Geosci* 336(4–5):455–466
- Sultan N, Delage P, Cui Y (2002) Temperature effects on the volume change behaviour of boom clay. *Eng Geol* 64(2–3):135–145
- Sun A, Yang G, Yang Q, Qi M, Wang N, Ren Y (2022) Experimental investigation of thermo-mechanical behaviors of deep-sea clay from the south china sea. *Appl Ocean Res* 119:103015
- Tang F, Lahoori M, Nowamooz H, Rosin-Paumier S, Masroufi F (2021) A numerical study into effects of soil compaction and heat storage on thermal performance of a horizontal ground heat exchanger. *Renewable Energy* 172:740–752
- Tourchi S, Vaunat J, Gens A, Bumbieler F, Vu M-N, Armand G (2021) A full-scale in situ heating test in callovo-oxfordian claystone: observations, analysis and interpretation. *Comput Geotech* 133:104045
- Towhata I, Kuntiwattanaku P, Seko I, Ohishi K (1993) Volume change of clays induced by heating as observed in consolidation tests. *soils and foundations* 33(4):170–183
- Vafaei N (2019) Experimental evaluation of sand-pile interface under monotonic and cyclic loads. PhD thesis, Amirkabir University of Technology (Tehran Polytechnic)
- Vafaei N, Fakharian K, Sadrekarimi A (2021) Sand-sand and sand-steel interface grain-scale behavior under shearing. *Transp Geotech* 30:100636
- Vasilescu R, Yin K, Fauchille A-L, Kotronis P, Dano C, Manirakiza R, Gotteland P (2019) Influence of thermal cycles on the deformation of soil-pile interface in energy pile. *E3S Web of Conferences*, Vol. 92, EDP Sciences, p 13004
- Wang H, Qi X (2020) Thermal volume change of saturated clays: a fully coupled thermo-hydro-mechanical finite element implementation. *Geomech Eng* 23(6):561–573
- Wang K, Shan Z, Wang M (2020) Undrained shearing behaviour of kaolin after undrained heating. *IOP Conference Series: Earth and Environmental Science*, Vol. 455, IOP Publishing, p 012102
- Wang K, Wang L, Hong Y (2020) Modelling thermo-elastic-viscoplastic behaviour of marine clay. *Acta Geotech* 15(9):2415–2431
- Wichtmann T, Fuentes W, Triantafyllidis T (2019) Inspection of three sophisticated constitutive models based on monotonic and cyclic tests on fine sand: hypoplasticity vs. sanisand vs. isa. *Soil Dyn Earthq Eng* 124:172–183
- Xiao S, Suleiman MT, McCartney JS (2014) Shear behavior of silty soil and soil-structure interface under temperature effects. *Geo-Congress 2014: Geo-characterization and Modeling for Sustainability*, pp 4105–4114
- Xiong H, Nicot F, Yin Z (2019) From micro scale to boundary value problem: using a micromechanically based model. *Acta Geotech* 14(5):1307–1323
- Xiong Y, Yang Q, Sang Q, Zhu Y, Zhang S, Zheng R (2019) A unified thermal-hardening and thermal-softening constitutive model of soils. *Appl Math Model* 74:73–84
- Yang G, Bai B (2019) Thermo-hydro-mechanical model for unsaturated clay soils based on granular solid hydrodynamics theory. *Int J Geomech* 19(10):04019115
- Yang G, Liu Y, Che P (2022) Thermal consolidation of saturated silty clay considering different temperature paths: Experimental study and constitutive modeling. *Int J Geomech* 22(3):04021293
- Yao Y, Zhou A (2013) Non-isothermal unified hardening model: a thermo-elasto-plastic model for clays. *Geotechnique* 63(15):1328
- Yazdani S, Helwany S, Olgun G (2019) Influence of temperature on soil-pile interface shear strength. *Geomech Energy Environ* 18:69–78
- Yin K (2021) Influence of clay fraction on the mechanical behavior of a soil-concrete interface. PhD thesis, École centrale de Nantes
- Yu H, Chen W, Gong Z, Ma Y, Chen G, Li X (2018) Influence of temperature on the hydro-mechanical behavior of boom clay. *Int J Rock Mech Min Sci* 108:189–197
- Zhou C, Ng CWW (2013) Experimental study of resilient modulus of unsaturated soil at different temperatures. In: *Proceedings of the 18th ICSMGE, Paris* (eds P. Delage, J. Desrues, R. Frank, A. Peuch and F. Schlosser) 2:1055–1058

Publisher's Note Springer Nature remains neutral with regard to jurisdictional claims in published maps and institutional affiliations.